Effects of J-gate potential and uniform electric field on a coupled donor pair in Si for quantum computing

Angbo Fang and Y. C. Chang
Department of Physics and Materials Research Laboratory, University of Illinois at Urbana-Champaign, Urbana, Illinois, 61801

J. R. Tucker
Department of Electrical Engineering, University of Illinois at Urbana-Champaign, Urbana, Illinois, 61801
(Received 4 March 2002; revised manuscript received 11 July 2002; published 30 October 2002)

We present theoretical studies of a coupled-donor pair in Si via an unrestricted Hartree-Fock method with a generalized valence bond wave function. Polarization properties and exchange coupling for a phosphorous donor pair in silicon under a J-gate potential (modeled by a parabolic well) and a uniform electric field (either parallel or perpendicular to the interdonor axis) are examined. The energies and charge distributions of the lowest-lying singlet and triplet states as functions of the J-gate potential and uniform electric field for various donor separations are analyzed. Implications for Si:P electron-spin-based quantum computer architecture are discussed.

DOI: 10.1103/PhysRevB.66.155331 PACS number(s): 03.67.Lx, 78.47.+p, 76.30.Lh

I. INTRODUCTION

The development of efficient quantum algorithms for classically difficult problems has generated an exploding interest in the construction of a quantum computer (QC).[1,2] Among dozens of quantum computer proposals, solid-state QC's are gaining popularity with their promise of scalability. In particular, quantum computer architectures implemented in semiconductors, where either electron spins[3] or nuclear spins[4] as qubits embedded in semiconductor structures have the potential to take advantage of the enormous resources of contemporary microelectronics. In such schemes, electron spins of localized electrons in semiconductors are used either as carriers of quantum information units (qubits) or as agents for coherent transfer of information between qubits realized on nuclear spins. By performing unitary transformations over arrays of qubits, data processing can be achieved in a quantum computer. It has been proved that any unitary multiqubit operation can be performed by the combination of single-qubit operations and the controlled-NOT two-qubit operation.[2] In most proposals for an electron-spin-based quantum computer, single-qubit operations are performed by bringing individual spins into resonance with applied magnetic fields, while two-qubit operations are implemented via an exchange interaction due to overlap of electron wave functions localized around neighboring sites. The exchange coupling between the two spins $\mathbf{S}_1$ and $\mathbf{S}_2$ is described by a Heisenberg Hamiltonian

$$H_{ex} = J\mathbf{S}_1 \cdot \mathbf{S}_2, \tag{1}$$

where J is the coupling strength, corresponding to the singlet-triplet splitting for the two localized electrons (labeled by 1 and 2). The effective exchange interaction [Eq. (1)] allows one to implement a ''square root of swap'' gate, $U_{SW}^{1/2}$, by applying a pulse $J(t)$ with $\int_0^{\tau_s} dt J(t)/\hbar = \pi/2 \pmod{2\pi}$. This gate, in combination with single-qubit gates, can realize any multiqubit operations.[5,6] For quantum dot electron-spin-based QC architectures, the typical switching time is around $\tau_s = 30$ ps, with the adiabatic pulse shape $J(t)$ height around $J_0 = 80$ μeV.[7,8]

In the initial state of a quantum computer, all qubits should be well isolated from one another. A two-qubit interaction is then switched on by an external gate. At the end of each complete operation, the two-qubit interaction is switched off again. One main obstacle in realizing accurate qubit operations is the electron-spin decoherence due to uncontrolled interaction with its surrounding environment. A reliable error-correction scheme[9] requires gate operations with an error rate no larger than one part in 10^4.[7,8,10] Fast but accurate gate control over qubits is therefore required. However, too fast mixing of the two-electron states would excite the previously frozen orbital degrees of freedom, which can lead to failure of the simplified Heisenberg Hamiltonian in the characterization of the low-energy dynamics of the two-electron system. It has been pointed out that adiabatic operation of the exchange gate can help reduce the errors caused by state mixing.[7,11] Thus, the optimum value of the gate operation time is constrained from below by the adiabatic condition and from above by the spin decoherence time. It is estimated[12] that the leakage rate of quantum information due to state mixing is reasonably small ($<10^{-6}$) for a gate operation time longer than 30 ps, for a typical coupled quantum dot QC system. In the Si:P spin-based architectures considered here, the single-donor energy-level spacing is larger than that for other types of quantum dots and the electron-spin decoherence time is much longer (as discussed below). Thus, we believe that the condition for adiabatic gate control would not lead to stringent requirements for quantum computing,[13] let alone the fact that there are nonadiabatic possibilities to perform gate operations.[14]

Conventionally, two parameters are used to approximately characterize the electron-spin decoherence: the direct electron-spin-flip time T_1 and the transverse spin lifetime T_2. Usually T_1 is larger than T_2. The switching time τ_s should be less than $10^{-4}T_2$ to make error-correction schemes reli-

able. For isotopically purified Si:P, T_2 is measured by spin-echo technique to be roughly 10^{-4} s to 10^{-3} s with a donor concentration $n=10^{16}$ cm^{-3}.[15,16] Here T_2 is mainly due to effects of the spin-orbit, multipole-multipole, and exchange interactions between neighboring electron spins. Kane pointed out that T_2 is probably limited by the dipolar interactions for very small donor concentrations.[17] In a quantum computer all these sources of decoherence can be regarded as controllable using compensating algorithms.[18,19] Compared with the lower bound of T_2 ($\sim$100 ns) observed in bulk GaAs using ultrafast time-resolved optical methods,[20] the electron-spin decoherence time in Si:P is much longer, and a Si:P-based QC would thus allow much slower gate control.

To describe the time evolution behavior of a system with a slowly time-dependent Hamiltonian, the adiabatic approximation can be employed. The state of a quantum system at time t can then be expanded as a linear combination of the instantaneous eigenstates at that time:[21] $\psi(t)=\Sigma_i c_i(t)u_i(t)$ and $H(t)u_i(t)=E_i(t)u_i(t)$. The time evolution of the coefficients $c_i(t)$ can be obtained by substituting these two equations into the time-dependent Schrödinger equation.

In a Si:P electron-spin-based QC scheme, donor ions act as labels for qubits (their corresponding bound-electron spins). Throughout a two-qubit gate operation, the lowest singlet state and triplet state should be well isolated from all other excited states to avoid leakage error in quantum computing.[8] A rough estimate of the typical donor (qubit) separation for a Si:P electron-spin-based QC can be done as follows. For a switching time of $\tau_s \sim 30$ ps, the peak value of the exchange coupling during a gate operation is around 0.08 meV. For error correction to be reliable, the exchange interaction at the off state must be less than 10^{-5} meV if we assume that the uncontrolled part of the interaction which induces decoherence has the same order of magnitude as the exchange interaction at the off state.

The asymptotic limit of the exchange energy between two hydrogenic systems separated by a distance R is given by[22]

$$J=1.64\frac{e^2}{\epsilon a_B}\left(\frac{R}{a_B}\right)^{5/2}\exp\left(\frac{-2R}{a_B}\right), \tag{2}$$

where a_B is the effective Bohr radius. Thus, an exchange energy of 10^{-5} meV corresponds to an interdonor separation of about 10 Bohr radii, or roughly 200 Å for two phosphorus donors. Such critical dimensions are well within the capability of today's scanning-tunneling microscopy lithographic technology.[23] Therefore, in this paper, we will concentrate our study on coupled donors separated by $R=8a_B$, $10a_B$, and $15a_B$, with a special emphasis on the $R=10a_B$ case.

In Kane's original proposal,[4] a J gate located between neighboring donors imposes an electrostatic potential to deform the electron wave functions and enhance the exchange coupling for two-qubit operations controlled by an adiabatic pulse. The ultimate goal is to find an optimal J-gate potential and time-dependent shape by considering its experimental feasibility and computing efficiency. This study of a coupled-donor pair under a static J-gate potential is intended to provide relevant information for experimental engineering of qubits and J gates, and may serve as a starting point for numerical simulation of the gate-controlled time evolution for a two-qubit system within the adiabatic approximation. External uniform field can also influence the energy difference between the singlet and triplet state by changing the effective Bohr radius of electrons bound to donors and the wave-function overlap. Their influence on the exchange splitting and charge distribution will reveal information about the decoherence due to uncontrolled gate-induced electric field and provide a means for the measurements of qubits.

In the past ten years the two-electron double quantum dot problem has been extensively studied due to its theoretical importance.[11,24–26] Hatree-Fock, Heitler-London, or Hund-Mulliken molecular-orbital methods were most often used to evaluate the lowest singlet and triplet energies. Qualitatively speaking, the reliability of these methods is strongly dependent on the specific system configuration and the trial wave function or basis set used. For example, the Heitler-London method would yield a ferromagnetic exchange coupling for hydrogenic systems separated by a very large distance ($\geqslant 60a_B$).[27] To the best of our knowledge, only qualitative evaluation or quantitative calculation with oversimplified models have been used to characterize the singlet-triplet splitting of localized electrons (either in coupled donors in a semiconductor environment or in coupled quantum dots) under uniform electric and magnetic fields.[11,24–26] Reliable quantitative calculations of the J-gate potential in the Si:P electron-spin-based quantum computing system has not yet been reported.

In this paper we introduce an unrestricted Hartree-Fock (UHF) method with a generalized valence bond (GVB) wave function to study the wave functions and eigenenergies for the lowest singlet and triplet states of the two-electron system under the influence of the J-gate potential and a uniform electric field parallel or perpendicular to the interdonor axis. In Sec. II we formulate our procedure for calculating the singlet and triplet states. We show that our method simplifies the two-electron problem to a single-electron problem while it accounts for (to a large extent) the electron correlation. The method gives better results than the regular Hartree-Fock method or Heitler-London approximation. In Sec. III, we model the effect of a J gate on the exchange coupling of an isolated donor pair with a parabolic potential. The effect of parallel and perpendicular electric field is discussed in Sec. IV. In Sec. V, we give a conclusion and address the implications of our results for Si:P electron-spin-based quantum computing.

II. UHF METHOD WITH GVB WAVE FUNCTION

The spatial Hamiltonian for two electrons bound to natural or artificial localization centers in semiconductor structures (e.g., shallow donors or quantum dots) can be written as

$$H(\mathbf{r_1},\mathbf{r_2})=H_1(\mathbf{r_1})+H_1(\mathbf{r_2})+v_{ee}, \tag{3}$$

where $H_1(\mathbf{r})$ is the Hamiltonian for one electron in the absence of the other electron and v_{ee} is the mutual Coulomb interaction. We write the two-electron spatial wave function

as a symmetric (singlet) or antisymmetric (triplet) combination of one-electron wave-function products,

$$\Psi_{\pm}(\mathbf{r_1},\mathbf{r_2}) = \frac{1}{\sqrt{2(1+S^2)}}[\phi_L(\mathbf{r_1})\phi_R(\mathbf{r_2}) \pm \phi_R(\mathbf{r_1})\phi_L(\mathbf{r_2})], \tag{4}$$

where the subscript $+(-)$ denotes singlet (triplet) states, ϕ_L (ϕ_R) denotes a one-particle wave function localized at the left (right) donor site, and $S \equiv |\langle \phi_L | \phi_R \rangle|$ is the overlap integral.

Our goal is to solve the Schrödinger equation

$$H(\mathbf{r_1},\mathbf{r_2})\Psi_{\pm}(\mathbf{r_1},\mathbf{r_2}) = E\Psi_{\pm}(\mathbf{r_1},\mathbf{r_2}). \tag{5}$$

UHF method is used to solve the lowest singlet and triplet states for the coupled-donor (quantum dot) system. Assume that in a given iteration, we already know the wave function $\phi_R(\mathbf{r})$. We choose an appropriate set of orthonormal basis functions, $b_n(\mathbf{r}); n = 1 \cdots N$ to describe the one-electron wave functions $\phi_L(\mathbf{r})$. Let the expansion coefficients for ϕ_L be L_n, and $R_n = \langle n | \phi_R \rangle$. The above two-electron eigenvalue equation can then be reduced to a single-electron eigenvalue problem by projecting it into the state ϕ_R. The projected eigenvalue equation within the basis now reads

$$\begin{aligned}\sum_n [&\langle n'|H_1|n\rangle + \langle \phi_R|H_1|\phi_R\rangle \delta_{n',n} \pm \langle n'|H_1|\phi_R\rangle R_n \\ &\pm R_{n'}\langle \phi_R|H_1|n\rangle + \langle n', \phi_R|v_{ee}|n, \phi_R\rangle \\ &\pm \langle n', \phi_R|v_{ee}|\phi_R, n\rangle]L_n = E\sum_n (\delta_{n',n} \pm R_{n'}R_n)L_n .\end{aligned} \tag{6}$$

Thus, $\phi_L(\mathbf{r})$ can be solved via the standard diagonalization procedure within the one-electron basis. The newly obtained $\phi_L(\mathbf{r})$ is then used to solve $\phi_R(\mathbf{r})$, and we do this iteratively until the singlet or triplet ground-state energies and wave functions converge.

For large donor (dot) separation (weak coupling), we may use the ground-state wave function of the single donor (atomic orbital) as our initial guess for either $\phi_R(\mathbf{r})$ or $\phi_L(\mathbf{r})$. For small donor (dot) separation (strong coupling), using the molecular orbital (MO) as our initial guess will work better. Since the donor ions are well separated in typical QC architectures, we will always use the atomic orbital as the starting point of our calculation.

The above forms of the singlet and triplet states are not the exact ones, but they are more general than either Heitler-London[28] (HL) or valence bond[29] wave function. Unlike the HL scheme which uses the fixed atomic orbitals of separated atoms, expression (4) employs flexible orbitals which are self-consistently optimized for the lowest two-particle energies in the subspace of singlet or triplet states. We have numerically verified that if we use the atomic orbital (molecular orbital) as the starting point for our unrestricted Hartree-Fock calculation, we get after one iteration a lower energy (both for singlet and triplet states) than that obtained by either the HL or MO approach. The wave function used here is characterized as a GVB wave function.[30] As compared to the single-determinant wave functions of restricted or unrestricted Hartree-Fock methods, our wave function given by Eq. (4) (after multiplying the corresponding singlet or triplet spinors) is a linear combination of two Slater determinants; thus, it represents a more accurate modeling of the real wave function beyond the regular mean-field approximation.

We note that for the triplet states

$$\begin{aligned}&\phi_L(\mathbf{r_1})[\phi_R(\mathbf{r_2}) + C\phi_L(\mathbf{r_2})] - [\phi_R(\mathbf{r_1}) + C\phi_L(\mathbf{r_1})]\phi_L(\mathbf{r_2}) \\ &\quad = \phi_L(\mathbf{r_1})\phi_R(\mathbf{r_2}) - \phi_R(\mathbf{r_1})\phi_L(\mathbf{r_2}),\end{aligned} \tag{7}$$

where C is an arbitrary constant. This means that if ϕ_L is linearly dependent on ϕ_R, we can always choose a new ϕ_L which is orthogonal to ϕ_R without altering the results. Numerically, since we use a finite set of basis functions, imposing such a constraint means we need to expand ϕ_L in terms of $N-1$ independent basis functions. Failure to do this will lead to a singular overlap matrix and the generalized eigenvalue problem will collapse. To avoid this problem, we use one less basis function for the expansion of $\phi_L(\mathbf{r})$ and require all basis functions to be orthogonal to $\phi_R(\mathbf{r})$ during each iteration.

We now apply the UHF method to solve the coupled phosphorous donor pair in silicon. Since the crystal environment makes the two-electron problem very complicated, we simplify the realistic Hamiltonian to a hydrogen-moleculelike Hamiltonian for the envelope function by ignoring the interband mixing and multivalley effect while assuming that the effects of the periodic crystal potential are captured by the effective-mass tensor and the background dielectric constant. Under such approximation the single-particle term H_1 can be simplified to the usual one-band effective-mass equation in real space:[31]

$$\left[\sum_{i=1}^{3} \frac{\hbar^2}{2m_i^*}\frac{\partial^2}{\partial x_i^2} + V_{imp}(\mathbf{r})\right]F(\mathbf{r}) = (E - E_0)F(\mathbf{r}), \tag{8}$$

where V_{imp} is the effective impurity potential composed of the screened Coulombic potential and the so-called ''central-cell'' correction.

In this approximation the impurity wave function can be expressed as the product of an envelope function and the Bloch function at the band minimum:

$$\phi(\mathbf{r}) = F(\mathbf{r})\phi^0_{\mathbf{k}_0}(\mathbf{r}). \tag{9}$$

To get an estimate of the energy scale and charge distribution for the ground state of a single donor, we consider the spherical-effective-mass model. In this model we use an spherically averaged effective electron mass given by $m^* = (\frac{1}{3}m_l^{*-1} + \frac{2}{3}m_t^{*-1})^{-1} = 0.3m_0$ for Si and an isotropic effective dielectric constant $\varepsilon_s^* = 11.4$.

In the case of shallow donors we may first neglect the central-cell correction and retain only the Coulombic poten-

tial with the effective charge $Z^*=1$. Equation (8) then reduces to a hydrogenlike Schrödinger equation. We define the effective Bohr radius,

$$a_B=\frac{4\pi\varepsilon_s^*\hbar^2}{m^*e^2}=0.529\ \text{Å}\frac{\varepsilon_s^*}{m^*/m_0}\approx 20\ \text{Å} \tag{10}$$

and the effective Rydberg (donor binding energy),

$$\text{Ry}^*=\frac{e^4m^*}{2\hbar^2\varepsilon_s^{*2}}=13.59\quad \text{eV}\frac{m^*/m_0}{\varepsilon_s^{*2}}\approx 30\ \text{ meV}. \tag{11}$$

Throughout the paper, we will use the effective atomic units (a.u.) in which distance is measured in a_B and energy measured in Ry*.

The one-particle Hamiltonian for the single-donor electron in Si:P can be described by a more realistic model Hamiltonian such as the one developed by Chang *et al.*[32] However, in this paper we shall adopt the spherical-effective-mass approximation for the following reasons. First, the results obtained in the spherical model can be directly compared with previous calculations at various limits to check the accuracy of the numerical method. Second, the spherical model calculation can be applied to not just Si, but many other systems involving coupled hydrogenic impurities. Third, the predictions made with this approximation will remain qualitatively correct when applied to realistic systems such as coupled phosphorous donors in Si.

III. EFFECTS OF J-GATE POTENTIAL

The potential imposed by a realistic J gate depends on the detailed experimental setting and can be rather complicated. Here, we model the J gate qualitatively by a one-dimensional parabolic potential with the minimum located in the middle of the two donor ions, which acts like an attractor and strongly enhances the wave-function overlap of the two donor electrons. The x axis passes through the two donor ions and their midpoint is at $x=0$. The effect of the J-gate potential takes the form $V_J=\mu(x-R/2)(x+R/2)/(R/2)^2$, where R is the separation between the two donor ions and μ is the energy difference (in units of Ry*) between the potential minimum (at $x=0$) and at donor sites ($x=\pm R/2$).

For convenience in choosing a finite set of flexible basis functions along the x axis, we place the system in a well with an infinite potential barrier for $|x|>L/2$. The size of L is chosen to be large enough (at least $5a_B$ from either donor ion), so it has negligible effect on the donor binding energy. We expand the spatial part of the single-particle wave function in terms of a linear combination of basis functions of the form

$$b_{m,i}(\mathbf{r})=\sqrt{2/L}\,\sin[k_m(x+L/2)]\beta_n(y^2+z^2), \tag{12}$$

where $k_m=m\pi/L$ and $\beta_n(y,z)$ is set of orthogonal functions constructed from the two-dimensional (2D) Gaussian functions $\exp[-\alpha_i(y^2+z^2)]$. The set of Gaussian parameters $\{\alpha_i\}$ are optimized such that a linear combination of the 3D Gaussian functions $\exp[-\alpha_i r^2]$ best resembles the $1s$ wave function of a hydrogen atom.[33] Since the donors are well separated and their electron wave-function mixing happens mainly along the x direction, the wave function in the y and z directions should remain close to the $1s$ orbital of isolated donors; thus, several Gaussian functions should be good enough to describe them. In the x direction, there would exist several kinds of mixing of single-particle orbitals, such as the s-p hybridized state (one electron in the s orbital of donor 1 while the other in the p orbital of donor 2), p-p hybridized state, and doubly occupied states (both electrons bound to the same donor ions), which may become significant when a gate potential or a parallel electric field is applied. The set of plane-wave functions in the x direction is flexible and convenient enough to characterize all possible state mixings. The suitability of the basis functions used here is examined by comparing our numerical results to the exact results in various limits. For example, with five 2D Gaussian functions and 50 sine functions we obtain a single-donor ground-state energy of -0.998 Ry and the H_2 molecule ground state energy of -2.282 Ry, which is better than the results obtained with the Heitler-London approximation[28] (-2.231 Ry) or Hartree-Fock approximation[34] (-2.267 Ry).

We first consider the case with interdonor separation $R=10a_B$. The box size used to define the plane-wave basis in the x direction is set to be $L=20a_B$, and 5×50 basis functions (five Gaussian functions in the plane and 50 plane waves along the x axis) are used for solving Eq. (6). Using the UHF method described in Sec. II, we calculate the energies and wave functions for the lowest singlet and triplet states as functions of the strength of the J-gate potential (μ). We are only interested in cases where μ is below some critical value μ_c, beyond which the electrons can be delocalized from the donor ions and trapped by the J-gate potential well. In that case, the electrons' spatial wave functions would be qualitatively changed, a condition that must be avoided during a gate operation.

To find the critical value μ_c, we define an averaged one-dimensional charge distribution along the interdonor axis as

$$\rho(x)=\frac{\int dy\int dz\int d\mathbf{r_2}|\Psi(\mathbf{r},\mathbf{r_2})|^2}{\int d\mathbf{r}\int d\mathbf{r_2}|\Psi(\mathbf{r},\mathbf{r_2})|^2}. \tag{13}$$

The charge distribution $\rho(x)$ undergoes a significant change when μ exceeds μ_c. It is found that μ_c depends strongly on the interdonor separation. Large separation allows a relatively deep gate potential to enhance the exchange splitting while keeping the qualitative shape of charge distribution unchanged.

Figure 1 shows the exchange splitting, J as a function of the J-gate potential, μ for two different interdonor separations, $R=8$, and $R=10$. At $\mu=0$ and $R=10$, we obtain an exchange splitting of 1.07×10^{-6} Ry*, which is about half of the asymptotic result estimated by Eq. (2). The exchange splitting increases exponentially as we increase the strength of the gate potential μ. The exponential dependence of J on μ enables such a J gate to switch on and off the spin-exchange coupling between neighboring qubits efficiently. At

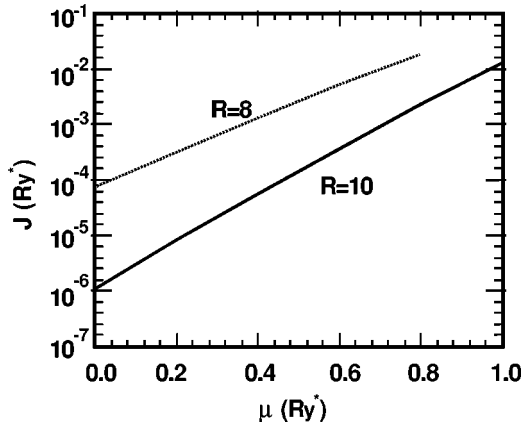

FIG. 1. Exchange splitting J as a function of the strength of J-gate potential μ for $R=8a_B$ and $10a_B$. We do not show the case of $R=15a_B$ here, because the exchange splitting (roughly 10^{-10} Ry*) at $\mu=0$ is smaller than the accuracy of our numerical calculation.

$\mu=0.8$ the exchange splitting is $J=0.0234$ Ry* (approximately 70 μeV if we use Ry*$=30$ meV) for $R=10a_B$. Such a value of exchange splitting is roughly the peak value of an adiabatic pulse shape $J(t)$ required to perform the two-qubit gate $U_{SW}^{1/2}$ during a switching time of $\tau_s \approx 30$ ps. We note that, at $R=15a_B$, the exchange splitting is about 10^{-10} Ry* when the J-gate potential is off (also consistent with the asymptotic result) while a gate potential with $\mu=1.0$ Ry* can only push the exchange energy to the order of 10^{-5}. This means that to complete a $U_{SW}^{1/2}$ operation, a quantum computer with qubit spacing $R=15$ will need about 30 ns, which is about 1000 times the time needed for $R=10a_B$.

Figure 2 shows the averaged charge distribution $\rho(x)$ for various strengths of the J-gate potential for $R=10a_B$. We see that up to $\mu=0.8$ Ry*, both electrons are still localized mainly around their donor ions in either the singlet or triplet state, while there is a significant charge buildup near $x=0$ as μ goes up to 1.0 Ry*. We note that $\rho(x)$ at $x=0$ in the singlet state is higher than its counterpart in the triplet state, as especially evident in Fig. 2 for the $\mu=1.0$ Ry* case. This can be understood based on the Pauli exclusion principle.

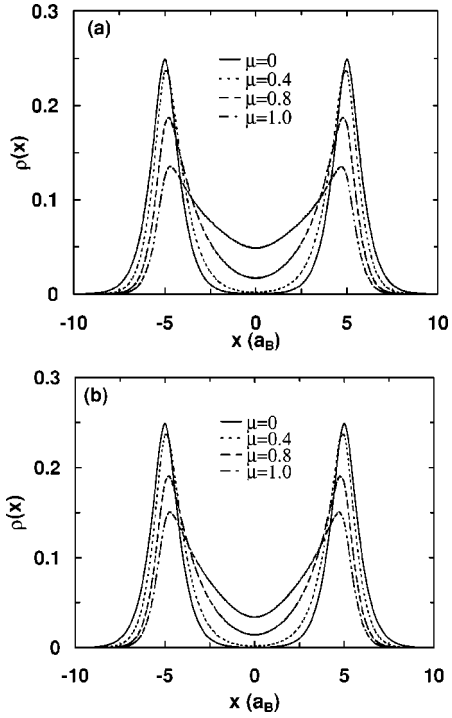

FIG. 2. Averaged charge distribution along the interdonor axis $\rho(x)$ [as defined by Eq. (13)] for various strengths of the J-gate potential. (a) Singlet; (b) triplet. The interdonor separation is fixed to be $R=10a_B$.

IV. EFFECTS OF UNIFORM ELECTRIC FIELD

To model the effects of a uniform electric field, we add an electrostatic potential term $V_F=eFx$ (eFz) for parallel (perpendicular) field to the Hamiltonian H_1, which leads to a Stark shift and finite lifetime for the (quasi-) bound states. We consider two cases: one with the electric field parallel to the interdonor axis (to study its effect on polarization) and the other perpendicular to the interdonor axis (to study its effect on exchange splitting).

A. Parallel field

For parallel field, the single-electron basis functions used are the same as those defined in the previous section [Eq. (12)]. Since the wave functions are confined in the region $|x|<L/2$, the problem of the electric-field-induced finite lifetime can be avoided. At finite field, the size of the confining box (L) must be chosen small enough so that the quantum confined energy level associated with the triangular potential introduced by the artificial confinement and the electric field is above the ground singlet or triplet state. Otherwise, the variational calculation will lead to an incorrect ground-state wave function. On the other hand, the confining walls cannot be placed within $5a_B$ to the closest donor ion in order to avoid an artificial quantum confinement effect on the exchange splitting. This consideration puts an upper limit on the strength of parallel field that can be applied before the variational calculation breaks down. However, this constraint can be relaxed if a finite J gate (a symmetric one-dimensional parabolic potential along the interdonor axis) is also present.

The Stark effect on the energies of the lowest singlet and triplet states is illustrated in Table I for $R=10a_B$ and $\mu=0$, where the width of the confining well is chosen to be ($L=20a_B$). The electric field lowers the energies of both singlet and triplet states, but the triplet state energy is much less affected due to the Pauli exclusion principle. We note that at $F=0.1$ Ry*$/a_B$, the singlet state becomes a doubly occupied donor state and the energy of the ground singlet state experiences an abrupt lowering compared to the energy at $F=0.08$ Ry*$/a_B$. If we further increase the electric field, the variational calculation will break down.

Next, we study the evolution of charge distributions of both singlet and triplet states at a fixed donor separation $R=10a_B$ in the presence of a fixed J-gate potential with strength $\mu=0.2$ Ry* as we vary the parallel electric field.

TABLE I. Energies for the lowest singlet (E_s) and triplet (E_t) states of a donor pair separated by $R=10a_B$ under a uniform electric field F along the interdonor axis. The exchange coupling is defined as the singlet-triplet splitting, $J=E_t-E_s$. All energies are in units of Ry* and the fields in units of Ry*/a_B. Note that the single-donor ground-state energy without applying electric field obtained in our variational calculation is $-0.997\,870\,87$ Ry*.

F	E_s	E_t	J
0	−1.995 742 79	−1.995 741 72	0.000 001 07
0.02	−1.996 605 58	−1.996 604 19	0.000 001 39
0.04	−1.999 212 69	−1.999 209 81	0.000 002 88
0.06	−2.003 626 54	−2.003 616 91	0.000 009 63
0.08	−2.010 076 07	−2.009 938 42	0.000 137 65
0.10	−2.194 618 38	−2.018 389 76	0.176 278 62

The confinement width is set to $L=30a_B$ and our basis consists of five radial Gaussian functions (in the y-z plane) and 80 sine functions of x (along the interdonor axis). We find that the singlet state changes abruptly to a doubly occupied state at a critical field due to the interplay of Stark shift and electron-electron interaction. Figure 3(a) shows the charge distribution of the ground singlet state along the x axis at zero field and in the neighborhood of the critical field. We see clearly that at an electric field less than 0.085 Ry*/a_B ($\sim$12.6 kV/cm), the charge density displays two distinct peaks centered around the two donor ions. The degree of distortion (polarization) is rather small, which indicates that the electric field is not large enough to conquer the Coulomb blockade. At $F=0.09$ Ry*/a_B, the singlet charge density displays a single enhanced peak (long-dashed curve) around the left donor ion, revealing an almost complete charge transfer from the right donor to the left.

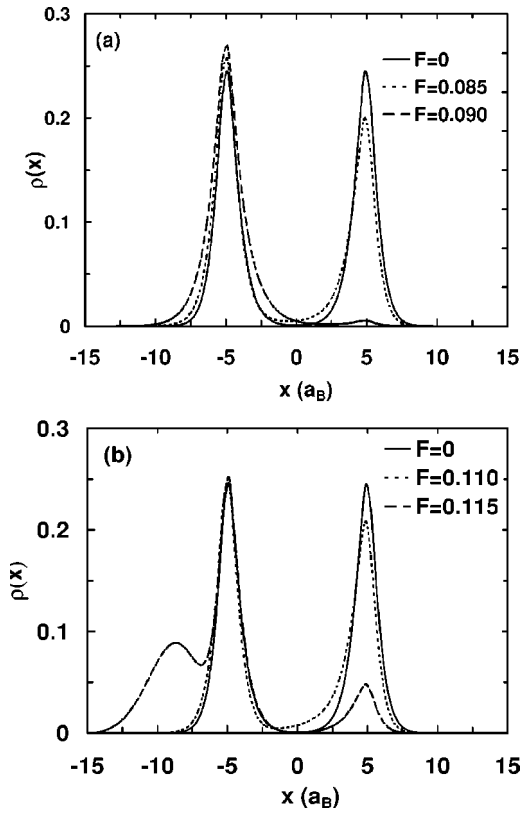

FIG. 3. Averaged charge distribution along the interdonor axis $\rho(x)$ for various strengths of the parallel electric field at a fixed donor separation $R=10a_B$ and J gate $\mu=0.2$ Ry*. (a) Singlet; (b) triplet.

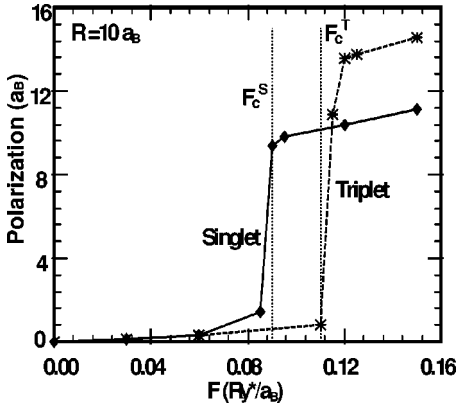

FIG. 4. The polarization of the lowest singlet and triplet states for $R=10$ and $\mu=0.2$. The critical fields for the singlet ($F_c^S=0.090$ Ry*/a_B) and triplet ($F_c^T=0.110$ Ry*/a_B) are marked with dotted perpendicular lines.

As shown in Fig. 3(b), the charge distribution of the triplet state as a function of the electric field is remarkably different from the singlet state. At $F=0.11$ Ry*/a_B, the charge distribution still displays two peaks similar to the $F=0$ case (other than a weak polarization indicating a slight charge transfer from the right donor ion to the region between two donor ions). This behavior again can be explained by the Pauli exclusion principle, which prevents the two electrons of parallel spin to reside on the same site. As we further increase the electric field to $F=0.115$ Ry*/a_B, the right donor is mostly ionized by the electric field and a new peak appears in the left region of the left donor, while the previous peak centered around the left donor remains unchanged. The appearance of the new peak indicates single-electron ionization of the two-donor molecule, which may be named ''Pauli-enhanced ionization.'' Compared to the triplet state, the doubly occupied singlet state is rather stable even under a large electric field with strength up to $F=0.2$ Ry*/a_B.

The polarizations (defined as the absolute expectation value of x_1+x_2, in units of a_B) for the lowest singlet and triplet states are plotted in Fig. 4 as functions of electric field for $R=10$ and $\mu=0.2$. There clearly exists a window between two critical electric fields, F_c^S (the field at which the singlet donor state abruptly changes to a doubly occupied donor state) and F_c^T (the field above which the lowest triplet state abruptly becomes ionized). Table II lists the values of critical electric fields for the singlet (F_c^S) and the triplet (F_c^T) for various donor separations and at different strengths of J gate. We found that the critical fields are insensitive to the strength of J gate, but sensitive to the donor separation. We note that the polarization behavior for the case with $R=8a_B$ and $\mu=0.4$ Ry* is qualitatively different and we find no abrupt change of the charge distribution. In this case, the

TABLE II. Strength of the critical electric fields (in Ry*/a_B) for the ground singlet state (F_c^S) at which the ground state becomes a doubly occupied state or the lowest triplet state (F_c^T) beyond which one donor electron is ionized.

R	$\mu=0.2$		$\mu=0.4$	
	F_c^S	F_c^T	F_c^S	F_c^T
8	0.105	0.150		
10	0.090	0.110	0.090	0.110
15	0.065	0.070	0.065	0.070

potential barrier between donor ions is significantly lowered and a new molecular orbital can be formed. The molecular orbital is a linear combination of atomic orbitals on the donor site and the localized orbitals centered at the bottom of the J-gate potential. This localized orbital acts like a bridge or relaxation channel for the charge transfer. As a result, the charge transfer occurs gradually as we increase the electric field. There is a high probability for one electron to stay on the bridge due to the interplay of the electric field and Coulomb blockade (or Pauli exclusion for the triplet state). It is pushed by the electric field from one side and blocked by Coulomb interaction (or Pauli exclusion) from the other side.

At a fixed donor separation, the critical electric field is different for singlet (F_c^S) and triplet (F_c^T) states, with $F_c^S < F_c^T$. Therefore, at an electric field with strength between F_c^S and F_c^T, where the singlet state is in a doubly occupied configuration while the triplet has not yet become ionized, the difference of their electron charge densities on the left half space is approximately 1. This fact can be used as an efficient means to distinguish the triplet state from the singlet state. Since the width of the window between the two critical fields for $R=10a_B$ is approximately $0.02\ \mathrm{Ry}^*/a_B \approx 3$ kV/cm, an accuracy of 1 kV/cm for the applied electric field is required for a readout scheme.

As shown in Table II, both F_c^S and F_c^T become smaller for larger donor separation. This can be understood as follows. For the singlet state, the potential-energy difference between the left and right donor sites due to the electric field is larger for the more widely separated donor pair, which makes it easier for the electron bound to the right donor to hop to the left donor site. For the triplet state, since the doubly occupied configuration is forbidden, one of the electrons tends to be more easily ionized at larger donor separation in order to keep the energy of the system lower. Burdov[35] derived an equation for the critical field of the singlet state of the two-electron double quantum dot based on a Hund-Mulliken ansatz:

$$\frac{1.786e^2}{\epsilon_s R}-\frac{e^2}{2\epsilon_s L}=2e|E|L, \tag{14}$$

where ϵ_s is the static dielectric constant, R is the dot radius, and $2L$ the interdot distance. The left-hand side of the equation is the energy difference between electron-electron interaction in the same and different quantum dots, and the right-hand side is the work done by the electric field on a charge to move it from one quantum dot to the other quantum dot. So, to do the same amount of work to overcome the Coulomb blockade (the left-hand side changes very little for a fairly large separation), the required field is smaller for larger donor (quantum dot) separation.

It has been proposed that the different polarization behavior of singlet and triplet states can be used as a means for measuring a single-electron spin state.[17,36] At the first step, the to-be-measured electron will be coupled to a second electron in a known spin state. Then a distinction of singlet or triplet of the two-electron system can be used to infer the spin state of the first electron. To measure whether the electrons are in a singlet or triplet state, the two-electron system will be put in the vicinity of the small island of a single-electron transistor (SET), whose conductance peaks (as a function of the chemical potential of the central island) will experience different shifts for singlet and triplet states, since their remarkably different polarizability will affect the island potential differently.

B. Perpendicular field

Using an electric field perpendicular to the interqubit axis to control the exchange coupling has also been considered. By using the Heitler-London ansatz and evaluating the difference of the Stark shift of mean positions of the two electrons, Burkard and co-workers[25] have shown that, in the case where dots of different sizes are coupled, such an electric field can switch the spin coupling on and off with exponential sensitivity. This semiquantitative argument cannot be applied to the case with bound electrons in Si:P acting as qubits, since such a perpendicular electric field will induce the same Stark shift for bound electrons which have the same Bohr radius.

Here we numerically calculate the dependence of the lowest-lying singlet and triplet energies on the strength of a uniform perpendicular electric field (taken to be along the z axis in our coordinate system). In this case, we expand the single-particle wave functions, $\phi_R(\mathbf{r})$ and $\phi_L(\mathbf{r})$, in terms of linear combinations of basis functions defined as

$$b_{m,\alpha_i,L}(\mathbf{r})=\sqrt{2/L}\,\sin[k_m(z+L/2)]e^{-\alpha_i[y^2+(x+R/2)^2]} \tag{15}$$

and

$$b_{m,\alpha_i,R}(\mathbf{r})=\sqrt{2/L}\,\sin[k_m(z+L/2)]e^{-\alpha_i[y^2+(x-R/2)^2]}, \tag{16}$$

respectively. The width of the confining well along the z direction is set to be $L=10a_B$. Six radial Gaussian functions (with optimized exponents) and 20 plane waves $\{\sqrt{2/L}\,\sin[k_m(z+L/2)]\}$ are used for the expansion of the single-particle wave functions.

Figure 5(a) shows how the exchange splitting varies as we increase the strength of the perpendicular electric field. For $R=10a_B$, the exchange splitting at $F=0.15\ \mathrm{Ry}^*/a_B$ is about 2.3 times the exchange splitting without the electric field. Figure 5(b) illustrates the dependence of electron wave-function overlap ($|\langle\phi_L|\phi_R\rangle|$) on the strength of perpendicular electric field. The electron wave-function overlaps for

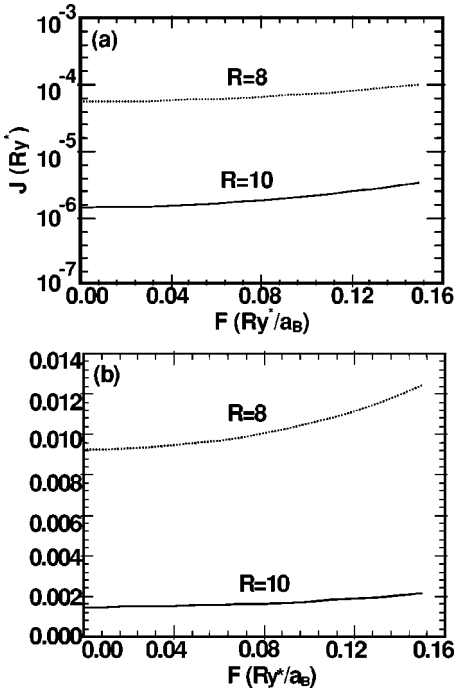

FIG. 5. (a) Exchange splitting and (b) electron wave-function overlap ($|\langle\phi_L|\phi_R\rangle|$) as functions of the perpendicular electric field for $R=10a_B$ and $R=8a_B$.

singlet and triplet states almost coincide, with the overlap for the singlet state slightly larger. As we increase the field, the wave-function overlap between the two electrons is enhanced. This is caused by the electric-field-induced s-p_z hybridization. Since the $2p_z$ orbital has a larger radius than the $1s$ orbital, the increased hybridization leads to a larger overlap. It is for this reason that the exchange splitting increases as the magnitude of the perpendicular electric field increases.

Although the exchange splitting does increase gradually with the increase of the field strength, we cannot use such a perpendicular electric field alone to switch on and off the spin coupling in a quantum computer since the electric field needed to produce the desired exchange splitting would be so large that the electrons would be well ionized from their donor sites. The field-ionization rate (in a.u.) of the ground-state hydrogen atom can be estimated according to the analytic formula[37]

$$\Gamma=(4/F)e^{-2/3F}. \tag{17}$$

At a field of 0.04 Ry*/a_B, the probability for ionization during a switching time of 30 ps is around 2.6×10^{-4}, which already exceeds the criterion for the error-correction scheme to work properly. At a field of 0.1 Ry*/a_B, the probability for ionization is already close to 100%. A more suitable scheme to manipulate the spin coupling in the coupled-donor system is to use the J gate as described in Sec. III, which does not have the problem of donor ionization.

V. CONCLUSION

In summary, we have calculated the exchange splitting for electrons bound to a donor pair in Si:P within a spherical-effective-mass approximation. By using the asymptotic formulas the approximate donor separation relevant for quantum computing is evaluated to be around $R=10a_B$, which is confirmed by our numerical calculation. We have used an unrestricted Hartree-Fock method with GVB wave functions to obtain the energies and wave functions for the lowest-lying singlet and triplet states of the coupled-donor system. Our method provides an efficient and reliable means by which to study two-center two-electron systems such as the double quantum dot and coupled-donor pair under external fields. Our method is better than the Heilter-London, Hund-Mulliken molecular-orbital, or regular Hartree-Fock approach.

Using a one-dimensional parabolic potential to simulate the effect of the J gate, we have studied the sensitivity of the exchange splitting to the gate potential. Our study confirms the feasibility of using such a J gate to switch on and off the spin-exchange interaction in a Si:P electron-spin-based quantum computer. Furthermore, we have analyzed the different polarizability of singlet and triplet states by numerically calculating the evolution of their charge distributions under a uniform electric field along the interdonor axis. We find that for a fixed donor separation there exists a window between two critical electric fields, within which the singlet state transforms to a doubly occupied configuration, while the triplet state remains in a bound coupled-donor state, thus displaying distinctly different polarizability. Such a finding provides a guide for the design of experiments for measuring the single-electron spin via the use of an SET, which senses the different polarizability in the singlet and triplet states. We have also studied the influence of a perpendicular electric field on the exchange splitting. We find that, although such an electric field does enhance the exchange splitting slowly by increasing the electron wave-function overlap, it cannot act as an efficient means by which to switch on and off the spin coupling.

Finally, we note that the current study has ignored the multivalley effect of the silicon conduction band and the central-cell correction of donor ions. Very recently Koiller *et al.*[38] examined the effect of intervalley electronic interference due to the existence of six conduction-band minima in Si, by revisiting the earlier work on magnetic susceptibility of the Si:P system.[39] Using linear combinations of envelope wave functions localized at the six equivalent valleys, they found that the intervalley scattering would lead to strong oscillations in the exchange splitting of neighboring donors.[38] Therefore, the position of donors should be precisely controlled. To give a more quantitative calculation of the exchange splitting for coupled donors in Si, one needs to apply a more realistic Hamiltonian,[32] and correspondingly, more realistic wave functions which treat electron correlation more completely, to study relevant issues that we have missed in this paper.

ACKNOWLEDGMENTS

This work was supported by the Defense Advanced Research Projects Agency (DARPA) under Contract No. DAAD19-01-1-0324.

[1] D. P. Divincenzo, Science **270**, 255 (1995); A. Ekert and R. Jozsa, Rev. Mod. Phys. **68**, 733 (1996).
[2] M. A. Nielsen and I. L. Chuang, *Quantum Computation and Quantum Information* (Cambridge University Press, Cambridge, England, 2000), and references therein.
[3] R. Vrijen, E. Yablonovitch, K. Wang, H. W. Jiang, A. Balandin, V. Roychowdhury, Tal Mor, and D. DiVincenzo, Phys. Rev. A **62**, 012306 (2000).
[4] B. E. Kane, Nature (London) **393**, 133 (1998).
[5] D. Loss, D. P. DiVincenzo, Phys. Rev. A **57**, 120 (1998).
[6] A. Barenco, C. H. Bennett, R. Cleve, D. P. DiVincenzo, N. Margolus, P. Shor, T. Sleator, J. A. Smolin, and H. Weinfurter, Phys. Rev. A **52**, 3457 (1995).
[7] J. Schlieman, D. Loss, and A. McDonald, Phys. Rev. B **63**, 085311 (2001).
[8] G. Burkard, H.-A. Engel, and D. Loss, Fortschr. Phys. **48**, 965 (2000).
[9] P. W. Shor, Phys. Rev. A **52**, R2493 (1995); A. M. Steane, Phys. Rev. Lett. **77**, 793 (1996).
[10] There are various estimates about the error tolerance of a quantum computer using error-correction codes, varying from 10^{-6} to 10^{-3}. See, for example, J. Preskill, Proc. R. Soc. London, Ser. A **454**, 793 (1998); C. Zalka, quant-ph/9612028 (unpublished). Most authors (Refs. 7 and 8) take the error tolerance as 10^{-4}.
[11] G. Burkard, D. Loss, and D. P. DiVincenzo, Phys. Rev. B **59**, 2070 (1999).
[12] X. Hu and S. Das Sarma, Phys. Rev. A **66**, 012312 (2002).
[13] For a recent study on the fault tolerance of adiabatic quantum computation, see, for example, A. M. Childs, E. Farhi, and J. Preskill, Phys. Rev. A **65**, 012322 (2002).
[14] For example, see C. Wellard, L. C. L. Hollenberg, and H. C. Pauli, Phys. Rev. A **65**, 032303 (2002).
[15] J. P. Gordon and K. D. Bowers, Phys. Rev. Lett. **1**, 368 (1958).
[16] M. Chiba and A. Hirai, J. Phys. Soc. Jpn. **33**, 730 (1972).
[17] B. E. Kane, Fortschr. Phys. **48**, 1023 (2000); (quant-ph/0003031 (unpublished).
[18] L. Viola, S. Floyd, and E. Knill, Phys. Rev. Lett. **83**, 4888 (1999).
[19] N. E. Bonesteel, D. Stepanenko, and D. P. DiVincenzo, Phys. Rev. Lett. **87**, 207901 (2001).
[20] J. M. Kikkawa and D. D. Awschalom, Phys. Rev. Lett. **80**, 4313 (1998).
[21] L. I. Schiff, *Quantum Mechanics* (McGraw Hill, New York, 1968).
[22] C. Herring and M. Flicker Phys. Rev. **134**, A362 (1964).
[23] J. L. O'Brien, S. R. Schofield, M. Y. Simmons, R. G. Clark, A. S. Dzurak, N. J. Curson, B. E. Kane, N. S. McAlpine, M. E. Hawley, and G. W. Brown, Phys. Rev. B **64**, 161401 (2001).
[24] X. Hu and S. D. Sarma, Phys. Rev. A **61**, 062301 (2000).
[25] G. Burkard, G. Seelig, and D. Loss, Phys. Rev. B **62**, 2581 (2000).
[26] E. B. Salem, S. Jaziri, and R. Bennaceur, Phys. Status Solidi B **224**, 397 (2001).
[27] C. Herring, *Direct Exchange Between Well-Separated Atoms*, in *Magnetism*, edited by G. T. Rado and H. Suhl (Academic Press, New York, 1966), Vol. IIB.
[28] H. Heitler and F. London, Z. Phys. **44**, 455 (1927).
[29] C. A. Coulson, *Valence* (Oxford University Press, London, 1961).
[30] C. Yannouleas and U. Landman, Eur. Phys. J. D **16**, 373 (2001).
[31] F. Bassani, G. Iadonisi, and B. Preziosi, Rep. Prog. Phys. **37**, 1099 (1974).
[32] Y. C. Chang, D. L. Smith, and T. C. McGill, Phys. Rev. B **23**, 4169 (1981).
[33] S. Huzinaga, J. Chem. Phys. **42**, 1293 (1965).
[34] D. R. Hartree, Proc. Cambridge Philos. Soc. **24**, 89 (1928); F. Fock, Z. Phys. **61**, 126 (1930).
[35] V. A. Burdov, Fiz. Tver. Tela. (St. Petersburg) **43**, 1110 (2001) [Sov. Phys. Solid State **43**, 1152 (2001)].
[36] B. E. Kane, N. S. McAlpine, A. S. Dzurak, R. G. Clark, G. J. Milburn, H. B. Sun, and H. Wiseman, Phys. Rev. B **61**, 2961 (2000).
[37] L. D. Landau and E. M. Lifshitz, *Quantum Mechanics: Non-Relativistic Theory*, 3rd ed. (Pergamon, New York, 1977).
[38] B. Koiller, X. Hu, and S. Das Sarma, Phys. Rev. Lett. **88**, 027903 (2002).
[39] K. Andres, R. N. Bhatt, P. Goalwin, T. M. Rice, and R. E. Wal, Phys. Rev. B **24**, 244 (1981).